Complex of B-DNA with Polyamides Freezes DNA Backbone Flexibility

Bernd Wellenzohn, Wolfgang Flader, Rudolf H. Winger, Andreas Hallbrucker, Erwin Mayer, and Klaus R. Liedl*

Contribution from the Institute of General, Inorganic and Theoretical Chemistry, University of Innsbruck, Innrain 52a, A-6020 Innsbruck, Austria

Received October 10, 2000. Revised Manuscript Received February 20, 2001

Abstract: The development of sequence-specific minor groove binding ligands is a modern and rapidly growing field of research because of their extraordinary importance as transcription-controlling drugs. We performed three molecular dynamics simulations in order to clarify the influence of minor groove binding of two ImHpPyPy-β-Dp polyamides to the d(CCAGTACTGG)$_2$ decamer in the B-form. This decamer contains the recognition sequence for the *trp* repressor (5′-GTACT-3′), and it was investigated recently by X-ray crystallography. On one hand we are able to reproduce X-ray-determined DNA−drug contacts, and on the other hand we provide new contact information which is important for the development of potential ligands. The new insights show how the β-tail of the polyamide ligands contributes to binding. Our simulations also indicate that complexation freezes the DNA backbone in a specific B_I or B_{II} substate conformation and thus optimizes nonbonded contacts. The existence of this distinct B_I/B_{II} substate pattern also allows the formation of water-mediated contacts. Thus, we suggest the $B_I \rightleftharpoons B_{II}$ substate behavior to be an important part of the indirect readout of DNA.

Introduction

Small polyamide molecules can bind in a sequence-specific way to the minor groove of B-DNA[1−13] and are therefore able to influence the expression of specific genes.[14−16] These ligands and other recently designed molecules with the potential to control transcription[17−19] are of great interest as antitumor, antiviral and antimicrobial agents.[20−33] Often a dimeric complexation of these ligands is observed.[34−36] In the case of the polyamides studied here, such a dimer binds in an antiparallel arrangement, by building specific contacts with the DNA. General pairing rules were developed, allowing the prediction of the specificity from the side-by-side pairing of aromatic pyrrole (Py), imidazole (Im), and hydroxypyrrole (Hp) amino acids. An antiparallel pairing of imidazole opposite pyrrole targets a G·C base pair, while the reversed pyrrole opposite imidazole recognizes a C·G pair.[2,11] A hydroxypyrrole/pyrrole

* Corresponding author.

(1) Urbach, A. R.; Szewczyk, J. W.; White, S.; Turner, J. M.; Baird, E. E.; Dervan, P. B. *J. Am. Chem. Soc.* **1999**, *121*, 11621−11629.
(2) Kielkopf, C. L.; White, S.; Szewczyk, J. W.; Turner, J. M.; Baird, E. E.; Dervan, P. B.; Rees, D. C. *Science* **1998**, *282*, 111−115.
(3) Kielkopf, C. L.; Baird, E. E.; Dervan, P. B.; Rees, D. C. *Nature Struct. Biol.* **1998**, *5*, 104−108.
(4) White, S.; Turner, J. M.; Szewczyk, J. W.; Baird, E. E.; Dervan, P. B. *J. Am. Chem. Soc.* **1999**, *121*, 260−261.
(5) Turner, D. *Curr. Opin. Struct. Biol.* **1996**, *6*, 299−304.
(6) Greenberg, W. A.; Baird, E. E.; Dervan, P. B. *Chem. Eur. J.* **1998**, *4*, 796−805.
(7) Herman, D. M.; Turner, J. M.; Baird, E. E.; Dervan, P. B. *J. Am. Chem. Soc.* **1999**, *121*, 1121−1129.
(8) Herman, D. M.; Baird, E. E.; Dervan, P. B. *Chem. Eur. J.* **1999**, *5* (3), 975−983.
(9) Swalley, S. E.; Baird, E. E.; Dervan, P. B. *J. Am. Chem. Soc.* **1997**, *119*, 6953−6961.
(10) de Clairac, R. P. L.; Geierstanger, B. H.; Mrksich, M.; Dervan, P. B.; Wemmer, D. E. *J. Am. Chem. Soc.* **1997**, *119*, 7909−7916.
(11) Wade, W. S.; Mrksich, M.; Dervan, P. B. *J. Am. Chem. Soc.* **1992**, *114*, 8783−8794.
(12) Mrksich, M.; Wade, W. S.; Dwyer, T. J.; Geierstanger, B. H.; Wemmer, D. E.; Dervan, P. B. *Proc. Natl. Acad. Sci.* **1992**, *89*, 7586−7590.
(13) Hawkins, C. A.; de Clairac, R. P.; Raymond, R. N.; Dominey, N.; Baird, E. E.; White, S.; Dervan, P. B.; Wemmer, D. E. *J. Am. Chem. Soc.* **2000**, *122*, 5235−5243.
(14) Gottesfeld, J. M.; Neely, L.; Trauger, J. W.; Baird, E. E.; Dervan, P. B. *Nature* **1997**, *387*, 202−205.
(15) Dickinson, L. A.; Gulizia, R. J.; Trauger, J. W.; Baird, E. E.; Mosier, D. E.; Gottesfeld, J. M.; Dervan, P. B. *Proc. Natl. Acad. Sci.* **1998**, *95*, 12890−12895.
(16) Wittung-Stafshede, P. *Science* **1998**, *281*, 657−658.
(17) Choo, Y.; Sanchez, I.; Klug, A. *Nature* **1994**, *372*, 642−645.
(18) Beerly, R. R.; Dreier, B.; Barbas, C. F., III. *Proc. Natl. Acad. Sci.* **2000**, *97*(4), 1495−1500.
(19) Dickinson, L. A.; Trauger, J. W.; Baird, E. E.; Dervan, P. B.; Graves, B. J.; Gottesfeld, J. M. *J. Biol. Chem.* **1999**, *30* (18), 12765−12773.
(20) Krugh, T. R. *Curr. Opin. Struct. Biol.* **1994**, *4*, 351−364.
(21) Neidle, S. *Biopolymers (Nucleic Acid Sci.)* **1997**, *44*, 105−121.
(22) Sen, S.; Nilsson, L. *J. Am. Chem. Soc.* **1998**, *120*, 619−631.
(23) Lane, A. N.; Jenkins, T. C.; Brown, T.; Neidle, S. *Biochemistry* **1991**, *30*, 1372−1385.
(24) Monaco, R. R.; Polkosnik, W.; Dwarakanath, S. J. *Biomol. Struct. Dyn.* **1997**, *15*, 63−67.
(25) Bifulco, G.; Galeone, A.; Nicolaou, K.; Chazin, W. J.; Gomez-Paloma, L. *J. Am. Chem. Soc.* **1998**, *120*, 7183−7191.
(26) Zakrzewska, K.; Lavery, R.; Pullman, B. *Nucleic Acids Res.* **1983**, *11*, 8825−8839.
(27) Ho, S. N.; Boyer, S. H.; Schreiber, S. L.; Danishefsky, S. J.; Crabtree, G. R. *Proc. Natl. Acad. Sci.* **1994**, *91*, 9203−9207.
(28) Patel, D. J. *Biochemstry* **1982**, *21*, 6424−6428.
(29) Perree-Fauvet, M.; Gresh, N. *J. Biomol. Struct. Dyn.* **1994**, *11*, 1203−1224.
(30) Walker, W. L.; Kopka, M. L.; Filipowski, M. E.; Dickerson, R. E.; Goodsell, D. S. *Biopolymers* **1994**, *35*, 543−553.
(31) Steinmetzer, K.; Reinert, K. E. *J. Biomol. Struct. Dyn.* **1998**, *15*, 779−791.
(32) Wemmer, D. E.; Dervan, P. B. *Curr. Opin. Struct. Biol.* **1997**, *7*, 355−361.
(33) Dervan, P. B. *Science* **1986**, *238*, 464−471.
(34) Gavathiotis, E.; Sharman, G. J.; Searle, M. S. *Nucleic Acids Res.* **2000**, *28*, 728−735.
(35) Wan, K. X.; Shibue, T.; Gross, M. L. *J. Am. Chem. Soc.* **2000**, *122*, 300−307.
(36) Gabelica, V.; Pauw, E. D.; Rosu, F. *J. Mass Spectrom.* **1999**, *34*, 1328−1337.

10.1021/ja003639b CCC: $20.00
Published on Web 05/05/2001

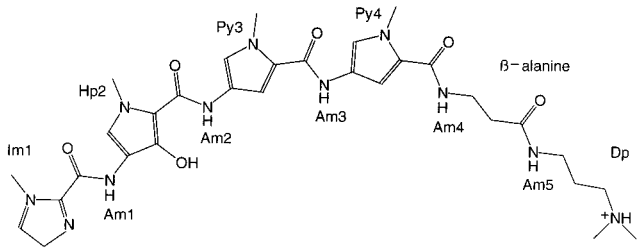

Figure 1. Chemical structure of the ImHpPyPy-*β*-Dp polyamide (Im, imidazole; Hp, hydroxypyrrole; Py, pyrrole; Am, amide; *β*, *β*-alanine; Dp, dimethylaminopropylamide). Numbering scheme is according to Kielkopf et al.[2]

pair is able to distinguish T·A from A·T base pairs. Recently, Kielkopf et al.[2] established the underlying structural basis by determining the crystal structure of the $d(CCAGTACTGG)_2$ decamer in the B-form complexed by two ImHpPyPy-*β*-Dp polyamides (see Figure 1; *β*, *β*-alanine; Dp, dimethylaminopropylamide). In contrast, the ImPyPyPy-*β*-Dp polyamides are not able to distinguish T·A from A·T.

The ImHpPyPy-*β*-Dp polyamides bind as an antiparallel dimer in the minor groove of the $d(CCAGTACTGG)_2$ DNA. The sequence specificity for T·A over A·T is explained by the formation of contacts with the asymmetric C2-cleft of adenine and with the double hydrogen bond acceptor potential of the thymine-O2.

Beyond direct base pair contacts, the conformational changes during ligand binding can be a major contributor to sequence-specific recognition processes. The roles of bending, unwinding, and other recognition tools in the indirect readout have been investigated extensively.[21,37−55] Backbone conformations of B-DNA such as B_I/B_{II} could be another important grammatical element in the recognition processes. The two substates B_I and B_{II} are defined by different conformations of the sugar phosphate backbone. In the B_{II} state, the phosphate group is rotated toward the minor groove (Figure 2).

The changes are best described by the ϵ and ζ angles of the DNA backbone or by the angle difference ($\epsilon - \zeta$). In the B_I state, the corresponding ϵ and ζ angles are between 120° and 210° (trans) and between 235° and 295° (gauche$^-$), respectively. For B_{II}, the ϵ angle lies between 210° and 300° (gauche$^-$), and ζ lies between 150° and 210° (trans).[56−58] The angle difference ($\epsilon - \zeta$) is close to −90° for B_I and +90° for B_{II} phosphates.[59] The existence of these substates was first pointed out by Gupta et al.[60] and later confirmed by different experimental and theoretical methods.[61−71]

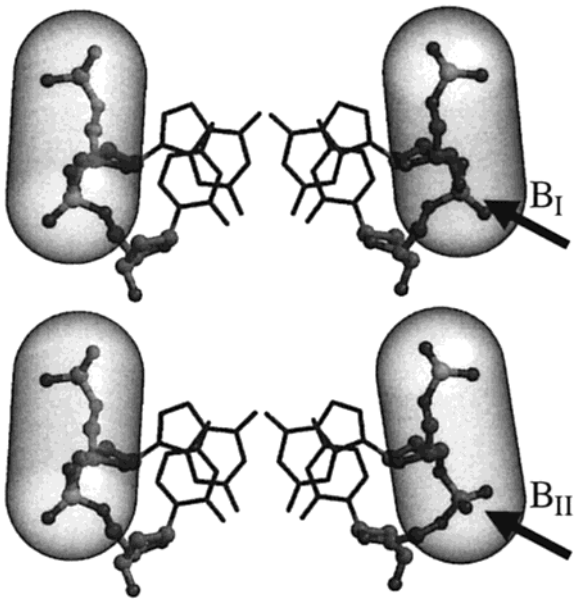

Figure 2. Side view of a base step in conformation B_I (top; the PO_2 group is approximately parallel to the base plane) and B_{II} (bottom; the PO_2 group is oriented normal to the base plane). The interconverting phosphates are marked by an arrow.

A high-resolution X-ray analysis of the $d(CCAGTACTGG)_2$ DNA[72] and the above-mentioned study of the $d(CCAGTACTGG)_2$−polyamide complex indicate that, despite entropic costs, ligand binding may stabilize a certain backbone conformation. An unusual B_{II} phosphate at the G4−T5 step was observed, and the B_{II} phosphates of P3 and P5 (numbering is according to Figures 7 and 8) are changed in the complex to B_I.

(37) Dickerson, R. E.; Chiu, T. K. *Biopolymers (Nucleic Acid Sci.)* **1998**, *44*, 361−403.
(38) Dickerson, R. E. *Nucleic Acids Res.* **1998**, *26*, 1906−1926.
(39) Giese, K.; Pagel, J.; Grosschedl, R. *Proc. Natl. Acad. Sci.* **1997**, *94*, 12845−12850.
(40) Chen, H.; Liu, X.; Patel, D. J. *J. Mol. Biol.* **1996**, *258*, 457−479.
(41) Shi, Y.; Berg, J. M. *Biochemstry* **1996**, *35*, 3845−3848.
(42) von Hippel, P. H. *Science* **1994**, *263*, 769−770.
(43) Strauss, J. K.; Roberts, C.; Nelson, M. G.; Switzer, C.; Maher, L. J., III. *Proc. Natl. Acad. Sci.* **1996**, *93*, 9515−9529.
(44) Bareket-Samish, A.; Cohen, I.; Haran, T. E. *J. Mol. Biol.* **1998**, *277*, 1071−1080.
(45) Wenz, C.; Jeltsch, A.; Pingoud, A. *J. Biol. Chem.* **1996**, *271* (10), 5565−5573.
(46) Steitz, T. A. *Structural studies of protein-nucleic acid interaction*; Cambridge University Press: Cambridge, UK, 1993.
(47) Lilley, D. M. J. *DNA−Protein: Structural Interactions*; Oxford University Press: Oxford, UK, 1995.
(48) Travers, A. *DNA−Protein Interactions*; Chapman & Hall: London, UK, 1993.
(49) Bewley, C. A.; Grinenborn, A. M.; Clore, G. M. *Annu. Rev. Biophys. Biophys. Chem.* **1998**, *27*, 105−131.
(50) Chen, Y.-Q.; Gosh, S.; Gosh, G. *Nature Struct. Biol.* **1998**, *5*, 67−73.
(51) Ellenberger, T. *Curr. Opin. Struct. Biol.* **1994**, *4*, 12−21.
(52) Gehring, W. J.; Qian, Y. Q.; Furukubo-Tokunaga, M. K.; Schlier, F.; Resendez-Perez, D.; Affolter, M.; Otting, G.; Wüthrich, K. *Cell* **1994**, *78*, 211−223.
(53) Harrison, S. C.; Aggarwal, A. K. *Annu. Rev. Biochem.* **1990**, *59*, 933−969.
(54) Neidle, S. *Oxford Handbook of Nucleic Acid Structure*; Oxford University Press: Oxford, UK, 1999.
(55) Pabo, C. O.; Sauer, R. T. *Annu. Rev. Biochem.* **1992**, *61*, 1053−1095.
(56) Schneider, B.; Neidle, S.; Berman, H. M. *Biopolymers* **1997**, *42*, 113−124.
(57) Berman, H. M. *Biopolymers* **1997**, *44*, 23−44.
(58) Hartmann, B.; Lavery, R. *Q. Rev. Biophys.* **1996**, *29*, 309−368.
(59) Fratini, A. V.; Kopka, M. L.; Drew, H. R.; Dickerson, R. E. *J. Biol. Chem.* **1982**, *257*, 14686−14707.
(60) Gupta, G.; Bansal, M.; Sasiskharan, V. *Proc. Natl. Acad. Sci* **1980**, *77*, 6486−6490.
(61) Privé, G. G.; Heinemann, U.; Chandrasegaran, S.; Kan, L.-S.; Kopka, M. L.; Dickerson, R. E. *Science* **1987**, *238*, 498−504.
(62) Cruse, W. B. T.; Salisbury, S. A.; Brown, T.; Cosstick, R.; Eckstein, F.; Kennard, O. *J. Mol. Biol.* **1986**, *192*, 891−905.
(63) Shindo, H.; Fujiwara, T.; Akutsu, H.; Masumoto, U.; Shimidzu, M. *J. Mol. Biol.* **1984**, *174*, 221−229.
(64) Sklenar, V.; Bax, A. *J. Am. Chem. Soc.* **1987**, *109*, 7525−7526.
(65) Gorenstein, D. G. *Chem. Rev.* **1994**, *94*, 1315−1338.
(66) Rüdisser, S.; Hallbrucker, A.; Mayer, E. *J. Am. Chem. Soc.* **1997**, *119*, 12251−12256.
(67) Bertrand, H. O.; Ha-Duong, T.; Fermandjian, S.; Hartmann, B. *Nucleic Acids Res.* **1998**, *26*, 1261−1267.
(68) Winger, R. H.; Liedl, K. R.; Rüdisser, S.; Pichler, A.; Hallbrucker, A.; Mayer, E. *J. Phys. Chem. B* **1998**, *102*, 8934−8940.
(69) Young, M. A.; Ravishanker, G.; Beveridge, D. L. *Biophys. J.* **1997**, *73*, 2313−2336.
(70) Cheatham, T. E., III; Kollman, P. A. *J. Am. Chem. Soc.* **1997**, *119*, 4805−4825.
(71) Pichler, A.; Rüdisser, S.; Mitterbock, M.; Winger, R. H.; Liedl, K. R.; Hallbrucker, A.; Mayer, E. *Biophys. J.* **1999**, *77*, 398−409.
(72) Kielkopf, C. L.; Ding, S.; Kuhn, P.; Rees, D. C. *J. Mol. Biol.* **2000**, *296*, 787−801.

We performed one molecular dynamics (MD) simulation of the complexed and two simulations of uncomplexed d(CCAGTACTGG)$_2$ decamer in order to investigate the influence of the polyamide complexation. As starting structure for the DNA complexed with the two ImHpPyPy-β-Dp polyamides, the X-ray structure from the Nucleic Acid Database[73] was used (NDB ID = BDD002).[2] The X-ray data of the uncomplexed d(CCAGTACTGG)$_2$-DNA (NDB ID = BD0023)[72] and the structure of the DNA in the complex were used as starting structures for the two MD simulations of the uncomplexed DNA.

Analyses of the resulting conformational behavior throughout the simulations indicate that complexation suppresses $B_I \rightleftharpoons B_{II}$ substate transitions, which is in agreement with the above-mentioned observation of the stabilization of a certain backbone conformation.[72] Thus, stable B_I/B_{II} backbone conformations seem to optimize nonbonded interactions and enable the formation of water-mediated contacts, supporting the influence of the backbone substates for the recognition process. These water-mediated contacts target the β-Dp tails of the polyamides, enabling an effect on binding in a way that has not been (to the best of our knowledge) observed before.

The polyamide−DNA hydrogen bonds of the X-ray structure are found to be stable during the whole simulation, but at the β-Dp tails the polyamide molecules exhibit the greatest flexibility, resulting in conformational transitions. These transitions provide new DNA−ligand contact information. Together with the above-mentioned water-mediated backbone contacts, they may be important for the design of new DNA targeting drugs.[13]

Methods

The simulation of biologically interesting molecules such as DNA[74−77] and DNA−ligand complexes has proven to be a valuable tool for a deeper understanding of structural and dynamical properties. An important advantage of MD simulations is the possibility to study dynamical effects. The inclusion of the long-range interactions via the Ewald summation in the form of the so-called particle mesh Ewald method allows the calculation of stable B-form DNA trajectories.[78−80] To take advantage of findings of previous extensive simulations,[69,81−83] protocols employed therein were directly adapted for our needs. We carried out three simulations as described below:

(A) As starting structure for the simulation of the d(CCAGTACTGG)$_2$-(ImHpPyPy-β-Dp)$_2$ complex, the crystal structure (NDB ID = BDD002) was used. Each strand of the DNA has nine PO_4^- anions, and each of the two polyamide ligands has one positive charge. To achieve electroneutrality, 16 Na^+ counterions were added using the program CION of the AMBER[84] package. Subsequently, solvation of the DNA with TIP3P Monte Carlo water boxes requiring a 12 Å solvent shell in all directions resulted in a system with dimensions 62.1881 × 47.1987 × 48.5762 Å^3, containing 3914 water molecules. The corresponding Γ value (water/nucleotide) is 195.7. The simulation was carried out using the AMBER5[84] package with the all-atom force field of Cornell et al.,[85] with the modifications by Cheatham et al.[86] The force field parameters for the polyamides were selected in analogy to existing parameters in the force field (available as Supporting Information). Charges were derived using the RESP[87] charge fitting procedure (multiconformational RESP). The ab initio electrostatic potential for RESP was calculated using GAUSSIAN94[88] at HF/6-31G* level of theory.

(B) As starting structure for the first simulation of the uncomplexed d(CCAGTACTGG)$_2$-DNA, the coordinates of the crystal structure from the DNA complex (NDB ID = BDD002) were used. Each strand of the DNA has nine PO_4^- anions, so 18 Na^+ counterions were added to achieve electroneutrality. The solvation of the DNA resulted in a box of dimensions 61.0420 × 48.6202 × 48.3249 Å^3, containing 3998 water molecules. The corresponding Γ value is 199.9. The simulation was carried out using the AMBER5[84] package with the all-atom force field of Cornell et al.,[85] with the modifications by Cheatham et al.[86]

(C) The starting coordinates for the second simulation of the free d(CCAGTACTGG)$_2$-DNA are from the crystal structure of the uncomplexed decamer (NDB ID = BD0023). The same procedure as for simulation B was employed, resulting in a box with dimensions 61.4806 × 47.0463 × 47.8060 Å^3 and a Γ value of 193.85.

Minimization/Equilibration. First, 500 steps of minimization were carried out with harmonic restraints of 25 kcal mol^{-1} Å^{-2} on DNA, counterion, and ligand positions. During the following five 100-step minimizations, the restraints on the counterions were relaxed faster than those on DNA and the ligand. Finally, 500 steps of unrestrained minimization were carried out. For the equilibration, a similar procedure was applied. After the constant volume system was heated over 10 ps from 50 to 300 K while the DNA and ion positions were kept constant, the harmonic restraints were reduced over the following 25 ps, on the counterions faster than on the oligonucleotide and ligand, using constant pressure and constant temperature conditions. Finally, 5 ps of unrestrained equilibration was carried out before the trajectory was generated for a further 2960 ps (simulation). The temperature bath coupling was achieved by using the Berendsen algorithm[89] (coupling constant = 0.2 ps for solute and solvent).

General simulation parameters were kept constant during the whole simulation: 2 fs time step, SHAKE constraints of 0.00005 Å on all bonds involving hydrogen atoms, 9 Å nonbonded cutoff, and 0.00001 convergence criterion for the Ewald part of the nonbonded interactions. The structural information was collected every 50 steps (0.1 ps). The resulting trajectory was analyzed with the carnal module of the AMBER5 package, and snapshots (collected every 200 ps) were investigated with different visualization programs.[90,91] Distances be-

(73) Berman, H. M.; Olson, W. K.; Beveridge, D. L.; Westbrook, J.; Gelbin, A.; Demeny, T.; Hsieh, S.-H.; Srinivasan, A. R.; Schneider, B. *Biophys. J.* **1992**, *63*, 751−759.

(74) von Kitzing, E. *Methods Enzymol.* **1992**, *211*, 449−467.

(75) Beveridge, D. L.; Ravishanker, G. *Curr. Opin. Struct. Biol.* **1994**, *4*, 246−255.

(76) Beveridge, D. L.; Swaminathan, S.; Ravishanker, G.; Withka, J. M.; Srinivasan, J.; Prevost, C.; Louise-May, S.; Langley, D. R.; DiCapua, F. M.; Bolton, P. H. Molecular Dynamics Simulations on the Hydration, Structure and Motions of DNA Oligomers. In *Water and biological macromolecules*; Westhof, E., Ed.; The Macmillan Press Ltd.: London, 1993; pp 165−225.

(77) Louise-May, S.; Auffinger, P.; Westhof, E. *Curr. Opin. Struct. Biol.* **1996**, *6*, 289−298.

(78) Cieplak, P.; Cheatham, T. E., III; Kollman, P. A. *J. Am. Chem. Soc.* **1997**, *119*, 6722−6730.

(79) Young, M. A.; Nirmala, R.; Srinivasan, J.; McConnell, K. J.; Ravishanker, G.; Beveridge, D. L.; Berman, H. M. Analysis of helix bending in crystal structures and molecular dynamics simulations of DNA oligonucleotides. In *Structural Biology*: *The State of the Art*; Adenine Press: Albany, NY, 1994; pp 197−214.

(80) Cheatham, T. E., III; Kollman, P. A. *J. Mol. Biol.* **1996**, *259*, 434−444.

(81) Young, M. A.; Jayaram, B.; Beveridge, D. L. *J. Am. Chem. Soc.* **1997**, *119*, 59−69.

(82) de Souza, O. N.; Ornstein, R. L. J. *Biomol. Struct. Dyn.* **1997**, *14*, 607−611.

(83) de Souza, O. N.; Ornstein, R. L. *Biophys. J.* **1997**, *72*, 2395−2397.

(84) Case, D. A.; Pearlman, D. A.; Caldwell, J. W.; Cheatham, T., III; Ross, W. S.; Simmerling, C. L.; Darden, T. A.; Merz, K. M.; Stanton, R. V.; Cheng, A. L.; Vincent, J. J.; Crowley, M.; Ferguson, D. M.; Radmer, R. J.; Seibel, G. L.; Singh, U. C.; Weiner, P. K.; Kollman, P. A. *AMBER 5*; University of California, San Francisco, 1997.

(85) Cornell, W. D.; Cieplak, P.; Bayly, C. I.; Gould, I. R.; Merz, K. M., Jr.; Ferguson, D. M.; Spellmeyer, D. C.; Fox, T.; Caldwell, J. W.; Kollman, P. A. *J. Am. Chem. Soc.* **1995**, *117*, 5179−5197.

(86) Cheatham, T. E., III; Cieplak, P.; Kollman, P. A. *J. Biomol. Struct. Dyn.* **1999**, *16*, 845−862.

(87) Bayly, C.; Cieplak, P.; Cornell, W.; Kollman, P. *J. Phys. Chem.* **1993**, *97*, 10269−10280.

(88) Frisch, M. J.; Trucks, G. W.; Schlegel, H. B.; Gill, P. M. W.; Johnson, B. G.; Robb, M. A.; Cheeseman, J. R.; Keith, T. A.; Petersson, G. A.; Montgomery, J. A.; Raghavachari, K.; Al-Laham, M. A.; Zakrzewski, V. G.; Ortiz, J. V.; Foresman, J. B.; Cioslowski, J.; Stefanov, B. B.; Nanayakkara, A.; Challacombe, M.; Peng, C. Y.; Ayala, P. Y.; Chen, W.; Wong, M. W.; Andres, J. L.; Replogle, E. S.; Gomperts, R.; Martin, R. L.; Fox, D. J.; Binkley, J. S.; Defrees, D. J.; Baker, J.; Stewart, J. P.; Head-Gordon, M.; Gonzalez, C.; Pople, J. A. *Gaussian 94*, Revision E.1; Gaussian, Inc.: Pittsburgh, PA, 1995.

(89) Berendsen, H. J. C.; Postma, J. P. M.; van Gunsteren, W. F.; DiNola, A.; Haak, J. R. *J. Chem. Phys.* **1984**, *81*, 3684−3690.

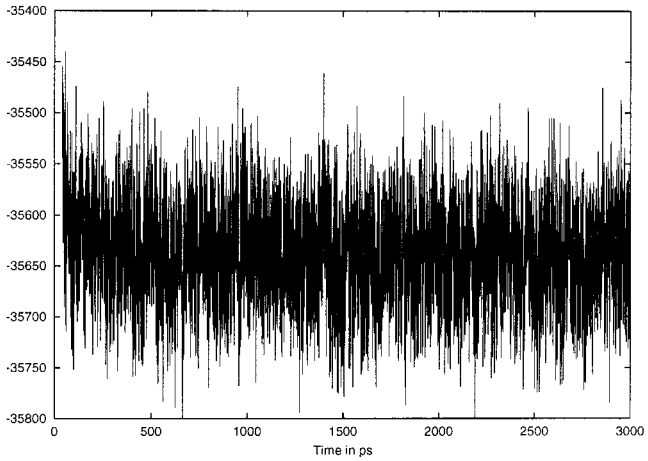

Figure 3. The graph indicates that the energy is stable during the simulation, which is a good indicator that equilibrium has been reached.

tween the heavy atoms (hydrogen bond acceptor and donor atoms) of 3.5 Å or less are interpreted as hydrogen bonds. A schematic description of the complex is given in Figure 6.

Results

Beyond the energy (Figure 3), which is stable during the whole simulations, the root-mean-square (rms) value is a good indicator that a system has reached equilibrium. Figure 4 demonstrates that the system reaches equilibrium very fast because after 500 ps no shift of the rms value is observable and only small fluctuations occur.

The mean value of the rms deviation for the whole complex is 1.88 Å, and it is 1.24 Å (Figure 4) for the ligands alone, which is in the range of a stable simulation. Thus, the polyamides exhibit a significantly larger flexibility than a previously investigated minor groove binder (netropsin: rms = 0.79 Å).[92] The β-Dp tails of the polyamide molecules show the greatest flexibility, resulting in a correlation between the rms deviation of the ligands and the contact distance between the positively charged nitrogen of the ligands and cytosine-O2 (not shown). Thus, the flexibility of the β-Dp tail, which is indicated by the distance plot, is the major contributor to the rms deviation of the ligands. Visual analysis of the trajectory with gOpenMol[91] and superpositions of the structures show that the transition is a 90° rotation of the $N^+(CH_3)_2$ group. In one conformation, both methyl groups are normal to cytosine2-O2 (Figure 5, right), and in the other conformation one methyl is directly between the cytosine2-O2 and the N^+, preventing close contact, presumably by steric hindrance (Figure 5, left). In the case of the close contact, the hydrogen of the protonated nitrogen is able to build a hydrogen bond. This bond may be important in order to stabilize the complex, but it cannot be responsible for sequence specificity, because all four possible base pairs have a hydrogen bond acceptor in this place of the minor groove.

Figure 5 show results from only one of the two dimeric bound ligands, but all mentioned results are valid for both ligands, as pointed out in Figure 6. The other freely rotatable single bonds of the flexible polyamide tails, surprisingly, exhibit no such distinctive conformer substate behavior.

Further analysis of the other DNA−ligand contacts reveals the above-mentioned high flexibility of the β-Dp tail of the polyamide and the rigidity of the ImHpPyPy part, because the contacts of the ImHpPyPy part are all stable with small standard deviations. Thus, only the tails of the ligands bind in a multimodal way to the DNA, and each polyamide tail interacts with the opposite DNA strand (Figure 6). The hydrogen bond lengths of the simulation and of the X-ray structure are listed in Table 1, showing that the X-ray-described hydrogen bonds can also be found in the simulation.

Although the simulation generally confirms the hydrogen bonds of the X-ray structure and thus no new binding mode is

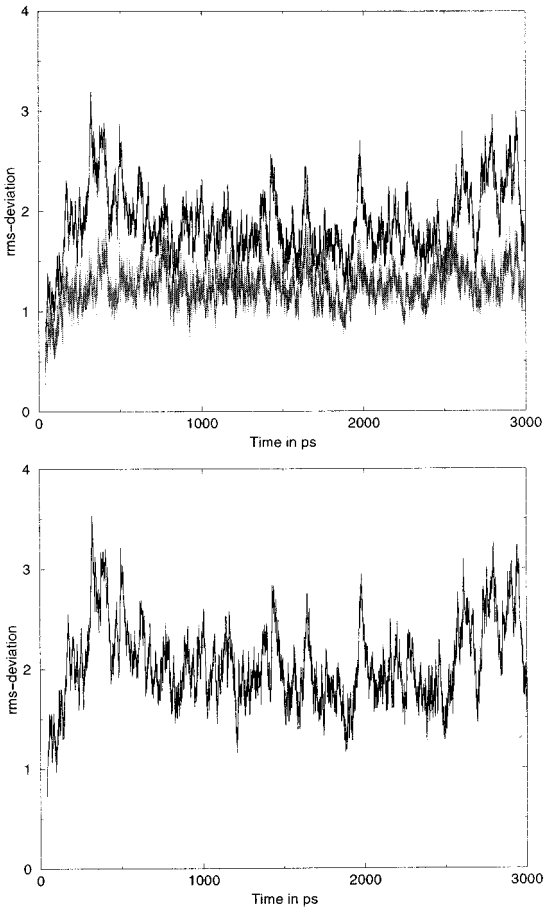

Figure 4. Rms deviation in angstroms with respect to the structure after the equilibration (top graph). The top curve describes the rms deviation of the complex (DNA and the two polyamide ligands), and the bottom curve is the rms value for the two ligands alone. The mean value of the top curve is 1.88 Å and that for the bottom curve is 1.24 Å. The bottom graph indicates the rms deviation with respect to the X-ray structure.

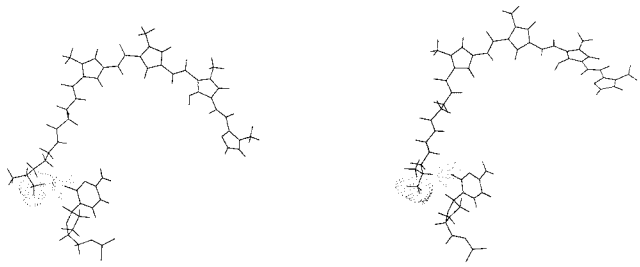

Figure 5. Structures of the two stable polyamide conformations. In the right structure, the two methyl groups of the positively charged nitrogen look away from the cytosine2-O2, thus allowing a short contact distance. In contrast, in the conformation of the left structure, one methyl is between the nitrogen and the O2 (indicated schematically by the van der Waals radius of the methyl group and O2) and prevents a close contact by steric hindrance. The pictures were made with rasmol.[90]

(90) Sayle, R.; Müller, A.; Bohne, A. *rasmol2.6ab9*; Molecular Modeling Group, German Cancer Research Center, 1999.
(91) Laaksonen, L. *gOpenMol 1.21;* Centre for Scientific Computing, Espoo (SF), 1996.
(92) Wellenzohn, B.; Winger, R. H.; Hallbrucker, A.; Mayer, E.; Liedl, K. R. *J. Am. Chem. Soc.* **2000**, *122*, 3927−3931.

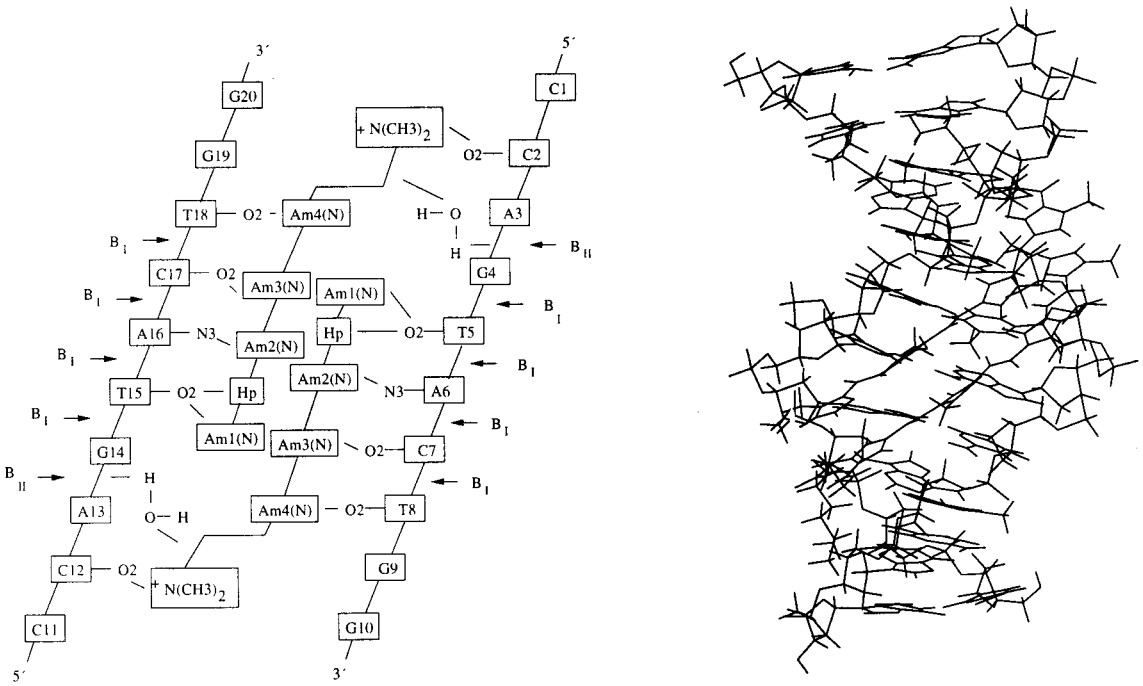

Figure 6. (Left(Schematic representation of the complex (the numbering scheme is referring to Figure 1) showing the hydrogen bond contacts of Table 1 and the other observed tail contacts (direct and water mediated). The phosphates, which are frozen in a particular B_I/B_{II} backbone substate, are indicated by arrows. The right structure is a snapshot (at 1.5 ns) from the simulation.

Table 1. Contact Distances between d(CCAGTACTGG)$_2$ and Ligand 1 (I.e., the Left ImHpPyPyβDp in the Schematic Representation of Figure 6) and Ligand 2 (I.e., the Right ImHpPyPyβDp in Figure 6)[a]

distances as indicated in Figure 6	X-ray ligand 1 (Å)	X-ray ligand 2 (Å)	simulation ligand 1 (Å)	simulation ligand 2 (Å)
Am1−N to T−O2	2.5	3.0	3.1	3.1
Am2−N to A−N3	3.2	3.8	3.3	3.4
Am3−N to C−O2	3.5	3.4	3.0	3.1
Am4−N to T−O2	3.1	3.1	3.0	3.0
Hp-O to T−O2	2.8	2.8	2.9	2.9
Hp-O to A−C2	3.5	3.4	3.8	3.8

[a] The values for the simulation are the mean values over the whole simulation, and the X-ray values are from Kielkopf et al.[3] The adenine of Hp-O to adenine-C2 and the thymine of Hp-O to thymine-O2 contact belong to the same A·T base pair. These Hp-O to adenine-C2 contacts are not indicated in Figure 6 because of the clarity of the schematic representation.

observed, the fine structure of the simulated complex differs in several ways from the experimentally determined data.[2] The hydrogen bonds of the hydroxypyrrole-OH (Hp-O) to the A·T base pair are of extraordinary interest because they allow the ligand to differentiate between A·T and T·A. So, our simulation suggests that the Hp-O to A-C2 hydrogen bond is longer (Table 1) and thereby less important than the above-mentioned publication[2] suggests. The differences between the solution and the crystal structure data cannot be assigned to one single transition; they rather result from deviations in the overall structure.

Recently, Kielkopf et al.[72] considered whether binding stabilizes a certain backbone conformation of the d(CCAGTACTGG)$_2$−polyamide complex. This local stiffening induced by drug binding, which results in unfavorable entropic costs, was observed several times and may play an important role in sequence specificity. We investigated the influence of drug binding on the $B_I \rightleftharpoons B_{II}$ transition behavior by simulating (molecular dynamics simulation) the complexed and uncomplexed DNA. As a starting point for the complexed system (simulation A), we used the X-ray structure. For the uncomplexed DNA we performed two simulations. As a starting point of the first uncomplexed DNA simulation, we only removed the ligands from the complexed DNA structure (simulation B), and the second simulation was started from the X-ray structure of the uncomplexed DNA (simulation C).

Figure 7 shows that, in contrast to the unbound DNA in the complexed DNA, almost no $B_I \rightleftharpoons B_{II}$ transitions occur in the complexed region. Thus, the polyamide dimer keeps the backbone in a particular conformation, thereby stiffening the DNA. It is worth mentioning that in the region in which the polyamides are in a dimeric arrangement, the B_I conformation is dominating, despite the observation that the B_{II} conformation widens the minor groove.[93] This is an indication that the effect of complexation on the $B_I \rightleftharpoons B_{II}$ behavior is not the result of steric hindrance, but rather is the result of an optimization of the nonbonded contacts. This explains how the entropic cost from the loss of the conformational freedom is compensated. Changes in the hydration of the grooves are known to be essential for B_I/B_{II} substate transitions.[68,94] The complexation of the DNA prevents the minor groove hydration, and thus these essential changes cannot occur, which may be another reason for the substate freezing.

To be sure that this result is not an artifact of the starting structure (the same complex structure for simulations A and B), we simulated the same sequence by using the X-ray structure[72] (NDB ID = BD0023) as starting structure (simulation C). This system exhibits a $B_I \rightleftharpoons B_{II}$ transition flexibility (Figure 8) comparable to that of simulation B. The phosphates are able to interconvert between the two substates, thus supporting the above-mentioned results of the DNA stiffening by complexation. A more detailed analysis of other structural aspects of simulations B and C will be given elsewhere.[95]

(93) Grzeskowiak, K.; Yanagi, K.; Privé, G. G.; Dickerson, R. E. *J. Biol. Chem.* **1991**, *266*, 8861−8883.

(94) Flader, W.; Wellenzohn, B.; Winger, R. H.; Hallbrucker, A.; Mayer, E.; Liedl, K. R. *J. Phys. Chem. B*, submitted.

(95) Wellenzohn, B.; Flader, W.; Winger, R. H.; Hallbrucker, A.; Mayer, E.; Liedl, K. R. *J. Phys. Chem. B* **2001**, *105*, 3135−3142.

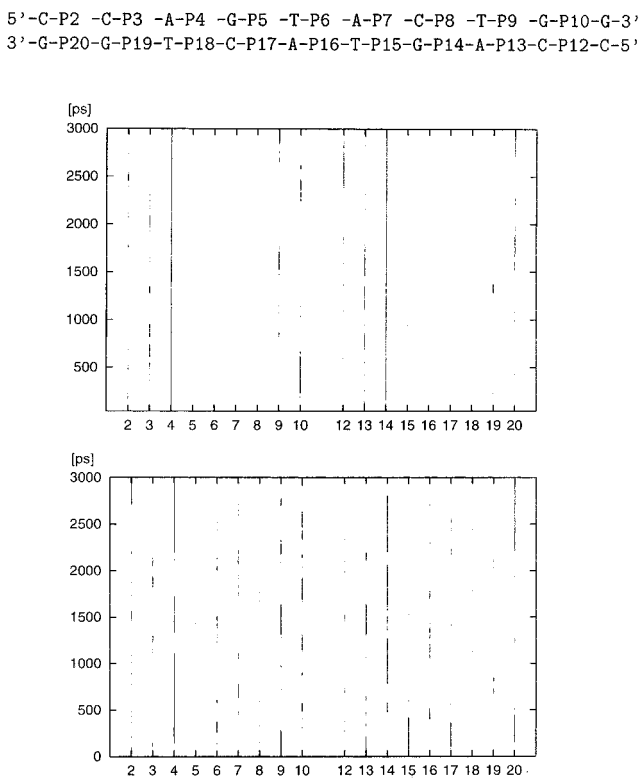

Figure 7. Conformational substates (B_{II}) as a function of time. The time the respective ($\epsilon - \zeta$) angle is in substate B_{II} is marked by a black line/dot. The top graph corresponds to the simulation of complexed DNA (simulation A), and the bottom picture describes the behavior of the uncomplexed DNA (simulation B). Enumeration of the interconverted phosphate groups is according to Kopka et al.[97] and is represented in the schematic description on the top.

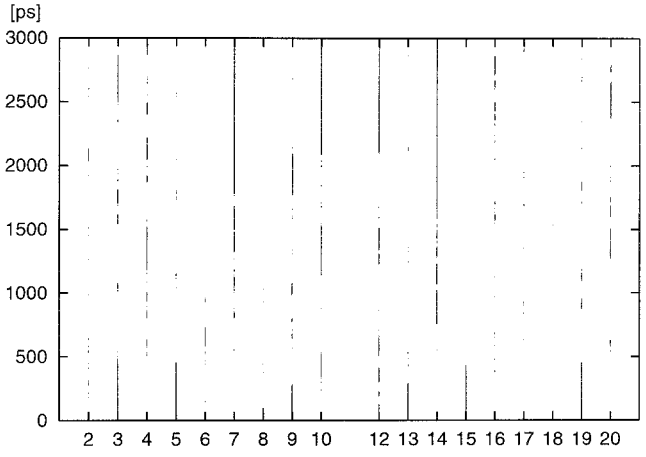

Figure 8. B_I/B_{II} substate behavior of simulation C. The phosphates of the complexed region are able to interconvert between both substates, indicating that the above-mentioned results are not an artifact of the starting structure.

The driving force behind the freezing of a particular substate may be the formation of better contacts between the ligand and DNA, but, through the particular $B_I \rightleftharpoons B_{II}$ conformation optimized, direct contacts are only one possible way this substate pattern can influence binding.

It is also conceivable that the conformational substate pattern influences water-mediated DNA−ligand bridges. Such water-mediated backbone contacts are already known to be important for sequence specificity in this recognition sequence.[96] The fourth and the fourteenth phosphates of the complex remain stable in B_{II} during the whole simulation. In this B_{II} conformation, one negative charged oxygen faces in the minor groove toward the tail of the ligand. Only this arrangement enables the formation of water-mediated contacts between the ligand and the phosphate oxygen. We analyzed snapshots of our trajectory and found that in 75% of the snapshots at least one water-mediated contact exists between the phosphate oxygens of P4 or P14 and the tail of the ligand (Figure 9). This water-mediated contact could explain why P4 and P14 are stabilized in B_{II} and demonstrates a second possibility of how the $B_I \rightleftharpoons B_{II}$ behavior can influence binding. Thus, our results give a new molecular insight into the important role of the polyamide tails for binding, being valuable in the design of new DNA targeting drugs.

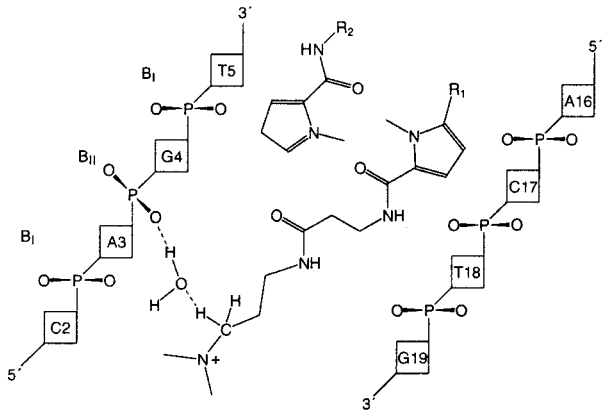

Figure 9. Schematic representation of the water-mediated contact (R_1 = ImHpPy, R_2 = HpPyPy-β-Dp). Distances between the hydrogen bond acceptor and donor (heavy atoms) of 3.5 Å or less can be interpreted as hydrogen bonds and are represented by a dashed line. For clarity, only one of the two possible contacts (P4 and P14) is indicated in this graph. In the B_{II} conformation, the phosphate group is rotated toward the minor groove, making the water-mediated contact possible.

Summary and Conclusion

We performed three MD simulations in order to investigate the effect of the complexation of the $d(CCAGTACTGG)_2$ decamer with two ImPyPyPy-β-Dp polyamides. Conformational transitions at the drug's termini were discovered, resulting in new contact information, which is useful for the design of new potential drugs. A detailed analysis of the effect on the $B_I \rightleftharpoons B_{II}$ substate behavior emphasized the possible importance of these substates in the recognition process. The DNA seems to adopt a particular substate in which the nonbonded contacts between drug and DNA are optimized. This indirect readout could also work through water-mediated contacts, as our simulation showed.

Acknowledgment. This work was supported by a grant from the Austrian Science Fund (Grant No. P13845-TPH).

Supporting Information Available: Atomic numbering scheme of polyamide; RESP charges and atomic types for the atoms of the polyamide complex; restraints on DNA and counterions during minimization and equilibration; AMBER atomic types used in the parametrization of the molecule; and AMBER atomic types used in the polyamide ligand (PDF). This material is available free of charge via the Internet at http://pubs.acs.org.

JA003639B

(96) Otwinowski, Z.; Schevitz, R. W.; Zhang, R.-G.; Lawson, C. L.; Joachimiak, A.; Marmorstein, R. Q.; Luisi, B. F.; Sigler, P. B. *Nature* **1988**, pp 321−329.

(97) Kopka, M. L.; Fratini, A. V.; Drew, H. R.; Dickerson, R. E. *J. Mol. Biol.* **1983**, *163*, 129−146.